ISPRS Journal of Photogrammetry and Remote Sensing xxx (xxxx) 1–12

Contents lists available at ScienceDirect

ISPRS Journal of Photogrammetry and Remote Sensing

journal homepage: www.elsevier.com/locate/isprsjprs

Radiative transfer modeling to measure fire impact and forest engineering resilience at short-term

José Manuel Fernández-Guisuraga[a,*], Susana Suárez-Seoane[b], Leonor Calvo[a]

[a] Area of Ecology, Faculty of Biological and Environmental Sciences, University of León, 24071 León, Spain
[b] Department of Organisms and Systems Biology (Ecology Unit) and Research Unit of Biodiversity (UO-CSIC-PA), University of Oviedo, Oviedo, Mieres, Spain

ARTICLE INFO

Keywords:
Burn severity
Deimos-2
Forest fire
Fractional vegetation cover
PROSAIL-D
Radiative transfer modeling
Resilience

ABSTRACT

Forest managers demand reliable and cost-efficient methodologies to implement forest resilience concepts in post-fire decision-making at different spatio-temporal scales. In this paper, we developed a generalizable remote sensing-based tool to measure disturbance impact and engineering resilience at short-term in forest ecosystems affected by wildland fires. The case study was a mixed-severity wildfire that burned several shrubland (dominated by gorse, broom and heath) and tree forest (dominated by oak and pine) ecosystems. Specifically, we retrieved fractional vegetation cover (FVC) over a time-series of pre and post-fire Deimos-2 imagery (spatial resolution of 4 m) from a radiative transfer model (RTM) hybrid inversion approach (Gaussian processes regression algorithm learned from a simulation dataset generated using the PROSAIL-D model). Pre and post-fire FVC retrieval was validated with field data stratified by dominant ecosystem. High accuracy (> 90%) and low error (< 7%) were achieved in the retrieval over the time-series, despite the influence of background signal of soil and burned legacies. A random point sampling stratified by ecosystem and burn severity was used to extract validated FVC values for the time-series. A two-way repeated measures ANOVA was performed to evaluate the effect of burn severity along the time-series on FVC for each ecosystem. One-way repeated measures ANOVA and Tukey's pairwise comparison test were applied to determine the earliest point in the time-series for which the FVC does not differ significantly from the pre-fire FVC. In tree forest ecosystems, the fire impact on FVC was stronger at high burn severity, being similar the impact on shrub ecosystems at medium and high burn severity. Engineering resilience was conditioned both by burn severity and species regenerative strategies. In ecosystems dominated by facultative or obligate seeders, pre-fire FVC was reached later across the time-series, compared to resprouter-dominated ecosystems. The RTM hybrid inversion tool has proved its reliability for assessing disturbance impact and ecosystem engineering resilience at short-term in heterogeneous fire-prone landscapes affected by mixed severity wildfires.

1. Introduction

Wildfires are major disturbances around the world (Chergui et al., 2019), playing a key role on the biological productivity, structure, composition and dynamics of many ecosystems (Calvo et al., 2008; Lozano et al., 2008; Pausas et al., 2008). In the western Mediterranean Basin, forest ecosystems have shown a great capacity to recover their structural characteristics to an equivalent pre-disturbance state under historical fire disturbance regimes (Keeley et al., 2011; Seidl et al., 2014; Johnstone et al., 2016). However, during the last century, abrupt shifts in Mediterranean ecosystems' fire regime (Pausas and Keeley, 2014a; Vilà-Cabrera et al., 2018) have occurred due to land use changes, associated to rural abandonment (Pausas, 2004; Sagra et al., 2019), and anthropogenic climate warming, both promoting the development of dense and dry fire-prone stands with a high fuel continuity. Consequently, the number of large high-severity wildfires have increased (Pausas and Fernández-Muñoz, 2012; González-De Vega et al., 2016; Chergui et al., 2018a; Sagra et al., 2019), resulting in altered biological legacies (i.e. biological structures that persist past disturbances; Franklin et al., 2000) that might hinder feedbacks that promote ecosystem resilience and, therefore, ecosystem recovery after fire (Seidl et al., 2014; Johnstone et al., 2016; Turetsky et al., 2017; Taboada et al., 2018).

* Corresponding author.
E-mail address: jofeg@unileon.es (J.M. Fernández-Guisuraga).

https://doi.org/10.1016/j.isprsjprs.2021.04.002
Received 22 January 2021; Received in revised form 23 March 2021; Accepted 5 April 2021
0924-2716/© 2021

Fire severity, defined as the loss of aboveground and belowground organic matter as a consequence of fire (Keeley, 2009), is one of the most crucial factors that shape ecosystem recovery trajectories in the early stages of succession (Bastos et al., 2011; González-De Vega et al., 2016). Ecosystem resilience is usually perceived as an indicator of the ecosystem response after the occurrence of a disturbance (Müller et al., 2016). Nevertheless two complementary perspectives on the concept of resilience have been identified (Newton and Cantarello, 2015; Müller et al., 2016; Ingrisch and Bahn, 2018): (i) "engineering resilience", defined as the time required for an ecosystem to return to its pre-disturbance state (Pimm, 1984); and, (ii) "ecological resilience", identified as the magnitude of disturbance that an ecosystem can absorb before changing its structure and function to an alternate stable state (Holling, 1973; Gunderson and Holling, 2002). Engineering resilience can be quantified using well-established metrics or simulation models to calculate the time required to reach the initial condition of that property (Martin et al., 2011; Ingrisch and Bahn, 2018). Besides that, ecological resilience is difficult to model and quantify (Grimm and Calabrese, 2011), since the concept relies on the existence of more than one stable state within the ecosystem being assessed (Newton and Cantarello, 2015), which is a hotly debated topic at present (Scheffer et al., 2001). In addition, ecological resilience measurements are based on indirect proxies (i.e. stakeholder assessments or case study comparison) derived from resilience theoretical aspects (Newton and Cantarello, 2015; Ingrisch and Bahn, 2018), which are largely context-dependent (Carpenter et al., 2005) and require long-term observations on a time scale appropriate to the ecosystem dynamics after disturbances (Scheffer et al., 2015).

Although field work methods are highly reliable for evaluating ecosystem recovery trajectories (Zhang et al., 2013; Merlin et al., 2015; González-De Vega et al., 2016), they are labor-intensive and time-consuming approaches when applied at a large scale (Fernández-Guisuraga et al., 2020). Hence, the synoptic nature of passive remote sensing earth observations offers nowadays an efficient way to achieve this goal (Veraverbeke et al., 2012), despite some constraints in specific ecosystems, such as multi-layered forests, where the reflectance signal captured by passive optical sensors is mostly determined by the structural properties of the top of the canopy (Healey et al., 2020). In such cases, the remote estimation of variables related to ecosystem vertical structure, or the horizontal structure of herbs, shrub and tree strata, might be limited to secondary correlations (Avitabile et al., 2012; Vogeler and Cohen, 2016). For instance, local texture computed from reflectance signal may be only sensitive to several canopy traits such as shadowing or moisture content, which are themselves proxies of sub-canopy forest structure (Healey et al., 2020). Traditionally, remote sensing studies on post-fire forest dynamics have been based on vegetation spectral indices (VIs), such as normalized difference vegetation index -NDVI- (e.g. Viedma et al., 1997; Yi et al., 2013; Ireland and Petropoulos, 2015), soil-adjusted vegetation indices -SAVIs- (e.g. Clemente et al., 2009; Vila and Barbosa, 2010) or Enhanced Vegetation Index -EVI- (e.g. Jin et al., 2012; Abdul-Malak et al., 2015), among others. Nevertheless, this approach requires the building of statistical relationships between local field data and VIs, so the results are site-specific (Chu et al., 2016) and not generalizable to other sites without a sound transferability analysis (Fernández-Guisuraga et al., 2019). Pixel unmixing models (e.g. spectral mixture analysis -SMA- and multiple endmember spectral mixture analysis -MESMA-) have also been commonly used to monitor post-fire recovery dynamics (e.g. Chu et al., 2016; Fernandez-Manso et al., 2016; Fernández-Guisuraga et al., 2020). This approach has a direct physical sense and its accuracy depends, to a large extent, on the precise delineation of representative spectral features (i.e. endmembers) of each post-fire ground components (Melville et al., 2019; Fernández-Guisuraga et al., 2020). However, the acquisition of pure endmembers with high confidence in burned landscapes with high spatial heterogeneity is a challenging task if very high spatial resolution remote sensing data are not available (Meng et al., 2017; Fernández-Guisuraga et al., 2019). An alternative to the previous methods is the use of physical methods based on the inversion of radiative transfer models (RTMs), which have received little attention for monitoring post-fire ecosystem dynamics. RTMs simulate the physical relationships between vegetation canopy reflectance and certain biophysical variables (e.g. leaf area index -LAI-, fractional vegetation cover -FVC- or leaf chlorophyll content -LCC-, among others) (Jia et al., 2016). Their inversion using observed optical satellite reflectance data can be exploited to retrieve the biophysical variable of interest to be used as a resilience indicator. Significantly, RTMs do not need to be parameterized with site-specific field data, which are usually unavailable at short or medium-term after fire (Darvishzadeh et al., 2008; Fernández-Guisuraga et al., 2021). In contrast to vegetation index or pixel unmixing model approaches, field data are only needed for retrieval validation purposes. Likewise, post-fire vegetation recovery trajectories could be monitored over large burned areas encompassing several ecosystems, since the physical relationships of RTMs are not site or ecosystem-specific (Yebra et al., 2008; Tao et al., 2019). Among the existing coupled leaf and canopy RTMs, PROSAIL (Jacquemoud et al., 2009) has been one of the most used methods for simulating vegetation canopy reflectance and the corresponding biophysical variables, due to its precision and fast computing time. Given the known ill-posed problem of RTM inversion (Yebra et al., 2008), indirect model inversion is usually performed through machine learning regression algorithms (MLRA; hybrid inversion), such as Neural Networks (Schlerf and Atzberger, 2006; Jia et al., 2016), randomForest (Wang et al., 2018; Tao et al., 2019) or Gaussian Processes Regression (Verrelst et al., 2015), due to their high precision and computational efficiency (Liang et al., 2015; García-Haro et al., 2018).

In this paper, we propose a reliable and generalizable management tool to be applied in burned ecosystems with different environmental characteristics, affected by different levels of burn severity, taking as case study a burned landscape of the western Mediterranean Basin. In the study site, ground spatial heterogeneity arises from two different aspects: the landscape comprises different shrubland and forest ecosystems and vegetation was burned at different severity levels. The approach is based on the assessment of disturbance impact and ecosystem engineering resilience at short-term with reference to FVC, retrieved over a time-series of pre and post-fire Deimos-2 imagery (spatial resolution of 4 m) using a RTM hybrid inversion approach (GPR algorithm learned from a simulation dataset generated using the PROSAIL-D RTM). FVC is defined as the green vegetation fraction of the considered land surface extension seen from the nadir (Jia et al., 2016; García-Haro et al., 2018; Fernández-Guisuraga et al., 2021). Dealing with passive remote sensing data, FVC actually quantifies the spatial extent of green vegetation at top of the canopy level in single and multi-layered ecosystems (Vogeler and Cohen, 2016). Thus, the considered resilience metric refers to the recovery of the green vegetation fraction seen from the nadir, regardless of the vegetation stratum.

To the best of our knowledge, RTMs have not been covered in the literature as a tool to assess disturbance impact and ecosystem resilience. Indeed, the analysis of how burn severity influences the resilience of different fire-prone ecosystems is a priority to improve management actions (Newton and Cantarello, 2015; González-De Vega et al., 2016) and determine the burn severity threshold that may exceed ecosystem resilience (Andrade et al., 2020). Nevertheless, resilience concepts have not been widely applied in forest management (Reyer et al., 2015), due to a lack of adequate methods to implement them (Nikinmaa et al., 2020). In this research, we adopted the concept of engineering resilience, based on the time required by the ecosystem to return to pre-disturbance FVC values, due to the next reasons: (i) We are interested in the evaluation of ecosystem resilience at short-term (less than five years) (Meng et al., 2015), which is restricted to the engineering resilience concept. (ii) FVC is one of the most typical and relevant engineering resilience indicators found in the literature (Nikinmaa et al., 2020), both for pre and post-fire forest management (Scheffer et al., 2015) and, especially, in the context of new fire disturbance regimes (Seidl et al., 2016).

2. Material and methods

2.1. Study site. Burn severity estimation

The case study is a mixed-severity wildfire that burned 9940 ha of shrublands and forests between 21th and 27th August 2017 in the Sierra de Cabrera mountain range (NW Spain; Fig. 1). The site has a rough and heterogeneous topography and the altitude ranges between 836 and 1938 m a.s.l. Soils are acidic and originated over siliceous lithologies (mainly slates in the north and quartzite in the south of the burned scar) (GEODE, 2019; ITACyL, 2019). Climate is Mediterranean temperate (García-Llamas et al., 2019), with average values of temperature and precipitation, for a 50-year period, of 9 °C and 850 mm, respectively, and two months of summer drought (Ninyerola et al., 2005). Wildfires are relatively frequent in the region (8.48 fires × 10 km^{-2} × 10 years^{-1}) and mainly of anthropic origin (García-Llamas et al., 2020). The target wildfire affected five types of ecosystems: on the one hand, shrublands dominated by either facultative seeders, as *Genista hystrix* Lange (gorse) and *Genista florida* L. (broom), or resprouter species as *Erica australis* L. (heath); on the other, forests dominated by the resprouter *Quercus pyrenaica* Willd. (oak) or the obligate seeder *Pinus sylvestris* L. (pine). In addition to that heterogeneity at landscape level, each ecosystem also presents a high spatial heterogeneity given local differences in post-fire regeneration patterns and accumulation of non-photosynthetic material derived from burning at different severity levels.

Two cloud cover-free Sentinel-2 MSI Level 1C scenes covering the burned scar were acquired from the Copernicus Open Access Hub () for both August 13th 2017 at 11:21:21 UTC (pre-fire) and 2nd September 2017 at 11:21:11 UTC (post-fire). The Level 1C product is already orthorectified by the image provider. The scenes were corrected for topographic and atmospheric effects to obtain a surface reflectance product at 10 m of spatial resolution with the ATCOR algorithm (Richter and Schläpfer, 2018) included in PCI Geomatica 2018 (PCI Geomatics Enterprises Inc.). MODIS water vapor product (MOD05) and meteorological data from the National Oceanic and Atmospheric Administration (NOAA) and the State Meteorology Agency of Spain (AEMET) were used to set the appropriate ATCOR input parameters. For both Sentinel-2 scenes, aerosol model was set to rural. Sub-arctic summer MODTRAN atmospheric model (water vapor content of 2.08 g cm^{-2}) was selected for the pre-fire scene, and a mid-latitude winter model (water vapor content of 0.85 g cm^{-2}) for the post-fire scene. Visibility value was fixed to 40 km for both scenes, which constitutes clear weather conditions. Remote sensing-based estimation of burn severity, considered as the total amount of biomass consumed (Keeley, 2009; Morgan et al., 2014), was computed through the differenced Normalized Burn Ratio (dNBR) index (Key, 2006) using surface reflectance data of band 8 (near infrared region) and band 12 (short wave infrared region) from the pre and post-fire Sentinel-2 processed scenes. The dNBR was se-

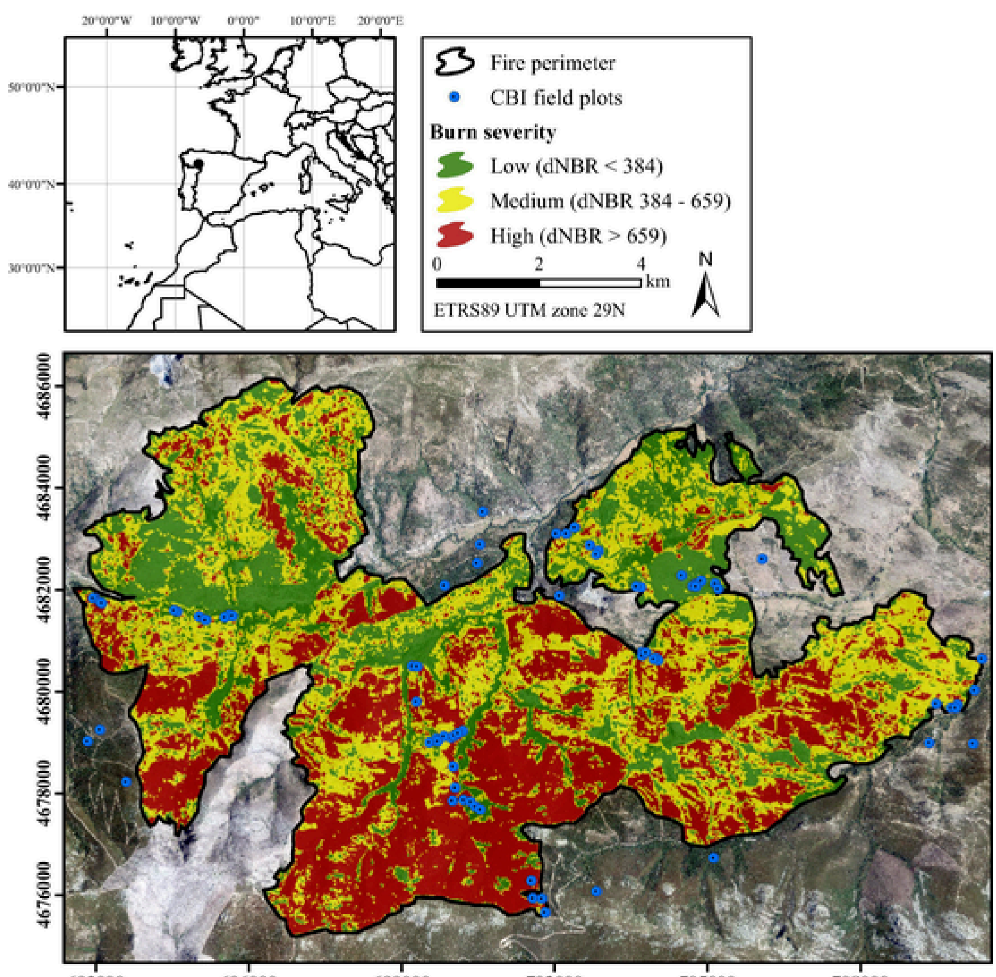

Fig. 1. Study site overview within the burned scar of the Sierra de Cabrera wildfire, location of the CBI field plots and estimated burn severity according to the difference of the Normalized Burn Ratio (dNBR) thresholds.

lected since it was the spectral index most related to field-based burn severity measures in the study site (García-Llamas et al., 2020), as well as determined by internal testing.

In order to validate the dNBR product, we established in the field, one month after the wildfire, a set of 53 plots of 30x30m that were georeferenced with a sub-meter accuracy GPS receiver. The plots were randomly distributed within the burned scar in homogeneous patches to ensure a uniform plot spectral signal to be registered by a 10 m Sentinel-2 MSI Level 2A pixel (Fernández-Guisuraga et al., 2021). We also established 19 unburned control plots within the outer burned scar. The Composite Burn Index (CBI; Key and Benson, 2006) was used to measure burn severity in each field plot using the modified protocol described in Fernández-García et al. (2018). Based on the CBI values, three field burn severity categories were recognized within the scar: low (CBI < 1.25), medium ($1.25 \leq$ CBI ≤ 2.25) and high (CBI > 2.25). Using the CBI thresholds, we established three dNBR burn severity categories by means of a linear regression model (Fig. 2): (low: dNBR < 384; medium: $384 \leq$ dNBR ≤ 659; high: dNBR > 659) (Fig. 1). The coefficient of determination was 0.84.

2.2. Remote sensing data and pre-processing

Deimos-2 is a multispectral imaging mission launched on 19th June 2014 and developed by Elecnor Deimos. Deimos-2 optical payload provides multispectral imagery at 4 m of spatial resolution in four bands over the visible (VIS) and near infrared (NIR) regions of the spectrum (Table 1).

Five Deimos-2 scenes were acquired during peak biomass of the study site in summer months between 2017 and 2020, in pre and post-fire conditions, to retrieve fractional vegetation cover and evaluate ecosystem resilience (Table 2). Specific acquisition dates were chosen on the basis of on-demand Deimos-2 imagery availability with the absence of cloud cover and as close as possible to the dates of interest. Deimos-2 scenes were already orthorectified by the image provider. As with Sentinel-2 imagery, Deimos-2 scenes were atmospherically and topographically corrected to obtain a surface reflectance product using the ATCOR algorithm (Richter and Schläpfer, 2018) bundled in PCI Geomatica 2018 (PCI Geomatics Enterprises Inc.). Same ancillary data as in Sentinel-2 atmospheric correction workflow were used to set the appropriate ATCOR input parameters for processing Deimos-2 imagery. Aerosol model was set to rural for each scene. Sub-arctic summer MODTRAN atmospheric model (water vapor content of 2.08 g cm^{-2}) was selected for scenes #1, #3 and #4 (Table 2), whereas a mid-latitude winter model (water vapor content of 0.85 g cm^{-2}) was chosen for scenes #2 and #3 (Table 2). Visibility value was fixed to 40 km for each scenes.

2.3. FVC retrieval from radiative transfer model (RTM) inversion

The coupled PROSPECT-D leaf optical model (Féret et al., 2017) and 4SAIL (Verhoef et al., 2007) canopy reflectance model, also known as PROSAIL-D, was used to simulate a training dataset of canopy spectral reflectance and the corresponding FVC. PROSPECT-D simulates hemispherical reflectance and transmittance of leaves from 400 to 2500 nm in the optical spectrum (Jacquemoud and Baret, 1990) as a function of specific physiological and biochemical variables (Féret et al., 2017): leaf structure parameter (N), leaf dry matter content (C_m), leaf equivalent water thickness (C_w), leaf chlorophyll content (C_{ab}), leaf carotenoid content (C_{ar}), leaf anthocyanin content (C_{ant}), brown pigment fraction (C_{bp}). 4SAIL simulates the spectral reflectance of turbid medium plant canopies (Jacquemoud et al., 2009) using as required variables the leaf reflectance and transmittance simulated by PROSPECT-D, as well as the next variables related to canopy structure and viewing and illumination conditions (Baret et al., 2007; Verhoef et al., 2007; Yebra and Chuvieco, 2009): leaf area index (LAI), average leaf angle (ALA), ratio between diffuse and direct radiation (skyl), hot spot effect (hspot), soil brightness factor (α_{soil}), solar zenith angle (θ_s), observation zenith angle (θ_o) and sun-sensor azimuth angle (φ). Fixed values and minimum and maximum boundaries for PROSPECT-D and 4SAIL input variables (Table 3) were derived from satellite scene metadata, literature review, the TRY database and field knowledge, considering the ecosystem variability of the study site (Baret et al., 2007; Kattge et al., 2011; Féret et al., 2017; Campos-Taberner et al., 2018; Wang et al., 2018; Tao et al., 2019). FVC in a turbid medium was computed using the classical gap fraction calculation (Eq. (1) and (2)) as a function of the simulated LAI and ALA at nadir observations (Jia et al., 2016; Wang et al., 2018).

$$P_0(\theta) = e^{-\lambda_0 \frac{G(\theta,\theta_1)}{\cos\theta} \times LAI} \quad (1)$$

$$FVC = 1 - P_0(0) \quad (2)$$

where $P_0(\theta)$ is the gap fraction at direction θ, $G(\theta,\theta_1)$ is the orthogonal projection of a unit leaf area along θ, being θ_1 the ALA. The variable λ_0 is the leaf dispersion. FVC is computed when θ is equal to 0 (nadir direction).

A Latin Hypercube Sampling algorithm (McKay et al., 1979) was implemented to generate 2000 samples within the RTM variable space defined by the minimum and maximum boundaries of each input variable (Table 3). This approach enables a significant decrease in the num-

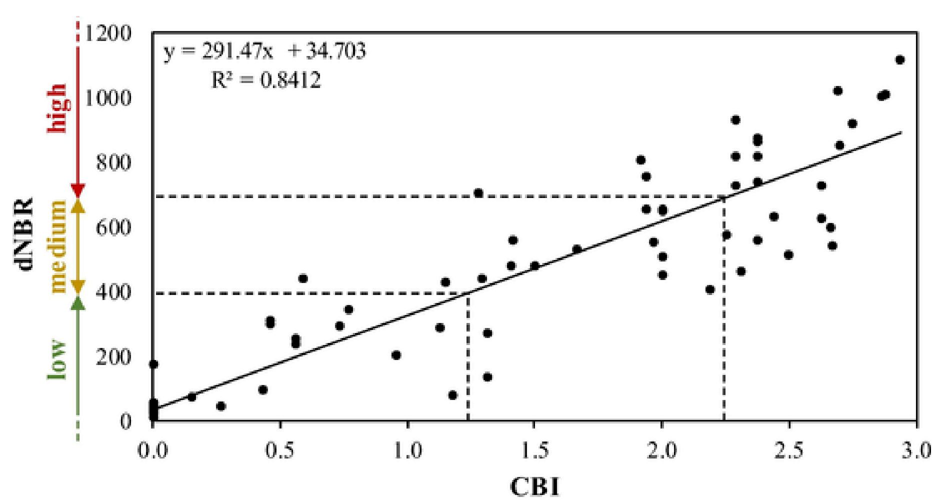

Fig. 2. Linear regression model used to compute dNBR thresholds (low-medium: dNBR = 384; medium-high: dNBR = 659) from CBI burn severity categories (low: CBI < 1.25; medium: $1.25 \leq$ CBI ≤ 2.25; high CBI > 2.25).

Table 1
Deimos-2 band configuration.

# Band	Region	Band center (nm)	Band width (nm)
1	blue	495.5	59
2	green	565.5	67
3	red	668.5	57
4	NIR	831	122

Table 2
Acquisition date of the Deimos-2 scenes used in the present study.

Scene #	Acquisition date	Date regarding fire
1	19th June 2017 10:14:44 UTC	2 months pre-fire
2	2nd September 2017 11:29:49 UTC	5 days post-fire
3	14th July 2018 10:52:10 UTC	1 year post-fire
4	30th June 2019 11:13:13 UTC	2 years post-fire
5	7th July 2020 10:58:15 UTC	3 years post-fire

Table 3
Fixed values and minimum and maximum boundaries of Latin Hypercube Sampling for PROSPECT-D and 4SAIL input variables.

PROSPECT-D leaf model	Symbol	Unit	Value or range
Leaf structure index	N	–	1.5–2.5
Leaf chlorophyll content	C_{ab}	$\mu g\ cm^{-2}$	20–90
Leaf dry matter content	C_m	$g\ cm^{-2}$	0.005–0.015
Leaf equivalent water thickness	C_w	$g\ cm^{-2}$	0.005–0.015
Leaf carotenoid content	C_{ar}	$\mu g\ cm^{-2}$	5–40
Leaf anthocyanin content	C_{ant}	$\mu g\ cm^{-2}$	0–40
Brown pigment fraction	C_{bp}	–	0–1
4SAIL canopy model	**Symbol**	**Unit**	**Value or range**
Leaf area index	LAI	$m^2\ m^{-2}$	0.1–6
Average leaf angle	ALA	°	30–80
Diffuse/direct radiation	skyl	–	0.1
Hot spot effect	hspot	–	0.001–1
Soil brightness factor	α_{soil}	–	0–1
Vegetation cover	V_{cov}	–	0–1
Solar zenith angle	θ_s	°	32.2
Observation zenith angle	θ_o	°	19.1
Sun-sensor azimuth angle	φ	°	42.6

ber of simulations required to completely map the variable space with respect to gridded or randomized sampling (Melendo-Vega et al., 2018), and typically, more than 500 samples as input to the RTM are enough to obtain reliable results (Vicent et al., 2018). The sampled simulations PROSAIL-D were run in forward mode to obtain a training dataset of simulated reflectance and the corresponding FVC. We added a relative white Gaussian noise of 2% to the simulated reflectances in order to account for RTM shortcomings and uncertainties of the atmospheric correction algorithm applied to observed satellite reflectance data (Jia et al., 2016; García-Haro et al., 2018). The simulations were spectrally resampled to Deimos-2 band configuration using a Gaussian model with full width at half maximum (FWHM) spacings (van der Meer and de Jong, 2001). To obtain realistic simulations in burned landscapes, the training dataset was finally updated with 20% of spectra representative of bare soil and charred woody debris with respect to the total model samples (García-Haro et al., 2018). Soil and woody debris spectra were extracted from the first post-fire Deimos-2 imagery.

Gaussian processes regression (GPR; Rasmussen and Williams, 2006) algorithm was used to model the relationship between the simulated Deimos-2 top of canopy reflectance and the corresponding FVC in the training dataset. GPR fits non-parametric and non-linear models described by a mean function and a radial basis function kernel (Verrelst et al., 2012a). Since GPR is based on a Bayesian probabilistic approach (Sinha et al., 2020), the model offers both the mean FVC prediction and the associated uncertainty (Verrelst et al., 2012a; Verrelst et al., 2016). GPR also yields slightly better biophysical parameter predictions than other machine learning regression algorithms (MLRAs) and is more computationally efficient (Verrelst et al., 2012b). The calibrated GPR model was then applied to Deimos-2 observed reflectance to obtain pixel-based mean FVC predictions and uncertainties (i.e. FVC retrieval).

PROSAIL-D parametrization, model run in forward mode and FVC retrieval through GPR were performed in ARTMO (Automated Radiative Transfer Models Operator) software (Verrelst et al., 2012c).

2.4. Field survey and retrieval validation

In September 2017 (the month following the fire event), 60 plots of 4 m × 4 m were established in the field within the fire scar to evaluate the performance of the FVC retrieval for the post-fire time-series. Additionally, 20 more plots were located in unburned areas next to burned ones to assess pre-fire FVC retrieval (unburned control plot approach; Díaz-Delgado et al., 2002). We equally stratified the field plots into four of the dominant ecosystems of the study site: (i) *Genista hystrix* gorseland (iii) *Genista florida* broomland (iii) *Erica australis* heathland and (iv) *Quercus pyrenaica* oak forest). The burned plots were also stratified by the three estimated burn severity categories. *Pinus sylvestris* plots could not be sampled due to accessibility problems and, therefore, FVC retrieval was not validated in this ecosystem. Deimos-2 pixel grid was used to ensure the alignment between the field plots and remote sensing data. The location of the field plots was measured using a sub-meter accuracy GPS receiver. Control and burned plots were both surveyed in September 2017, being burned plots also monitored in summer months of 2018, 2019 and 2020, following the protocol by Fernández-Guisuraga et al. (2021). We measured FVC in each plot as the vertical projected area occupied by each ecosystem stratum (i.e. herbs, shrub and tree layers), by means of a visual estimation method in steps of 5% (Anderson et al., 2005; Calvo et al., 2008; Delamater et al., 2012; Liang et al., 2012). The final FVC measure of each field plot was the average of the values given by four observers, being the standard deviation of the measures less than 5%. To deal with vertical strata in tall tree communities, a bottom-up direction was used to estimate the FVC of the tree canopy layer using a quadrat held by long sticks, being the FVC of the understory vegetation that can be viewed through canopy gaps estimated in a top-down direction (Mu et al., 2015; Jia et al., 2016). The coefficient of determination (R^2) and the root-mean-squared error (RMSE) was computed to measure the performance of the FVC retrieval on the basis of field data for the entire time-series.

2.5. FVC retrieval benchmarking

Three suitable vegetation indices (VIs) for the Deimos-2 band setup, and commonly used in the literature for predicting FVC (Vila and Barbosa, 2010; Ding et al., 2016; Younes et al., 2019), i.e., (i) Enhanced Vegetation Index (EVI), (ii) Modified Soil Adjusted Vegetation Index (MSAVI2) and (iii) Normalized Difference Vegetation Index (NDVI) (Table 4), were chosen for estimation of FVC using GPR, as a benchmark method of the FVC retrieval through RTM hybrid inversion. The performance of trained GPR models from field-measured FVC and VIs was evaluated by means of 5-fold cross-validation, averaging the R^2 and RMSE on each out-of-fold prediction. This benchmark method was selected because VIs are the most widely used method to evaluate post-

Table 4
Vegetation indices used as benchmark method and formulation for Deimos-2 band setup.

Index	Formula	Reference
EVI	$2.5\frac{\rho_4-\rho_3}{(\rho_4+6\rho_3-7.5\rho_1+1)}$	Gao et al. (2000)
MSAVI2	$\frac{2\rho_4+1-\sqrt{(2\rho_4+1)^2-8(\rho_4-\rho_3)}}{2}$	Qi et al. (1994)
NDVI	$\frac{\rho_4-\rho_3}{\rho_4+\rho_3}$	Rouse et al. (1979)

fire recovery trajectories in terms of FVC (Fernandez-Manso et al., 2016; Fernández-Guisuraga et al., 2020).

2.6. Data analysis

A random point sampling (Table 5), stratified by ecosystem and burn severity, was conducted within the fire scar to calculate the mean and standard deviation of FVC for each ecosystem and year across the time-series. We ensured a minimum distance of 100 m between points.

A two-way repeated measures ANOVA (2w-rmANOVA) was performed to evaluate the effect of burn severity along the time-series on the sampled FVC for each ecosystem. The interaction between burn severity and time was decomposed using one-way repeated measures ANOVA (1w-rmANOVA) at each level of burn severity, followed by a Tukey's pairwise comparison test to determine the significance of the differences between each point in the time-series. Following the definition of engineering resilience, the time required for FVC to reach pre-fire conditions, in each ecosystem and burn severity level, will be the earliest point in the post-fire time-series where FVC values do not differ significantly from pre-fire FVC. To facilitate the interpretation of the results, differences in the disturbance impact (magnitude of change between pre and immediate post-fire FVC) among burn severity levels in each ecosystem were assessed by means of a one-way ANOVA (1w-ANOVA), followed by a Tukey's pairwise comparison. Statistical significance was determined at $p < 0.05$. All statistical analyses were performed in R (R Core Team, 2019) with "rstatix" package (Kassambara, 2020).

Table 5
Random stratified point sampling per ecosystem.

ECOSYSTEM	Gorse	Broom	Heath	Oak	Pine
Burned area (ha)	888.84	1989.63	1779.30	1338.59	465.57
# Random points	170	380	340	256	89

3. Results

FVC retrieval from Deimos-2 imagery based on the GPR algorithm trained with PROSAIL-D canopy reflectance simulations featured a high accuracy and a low error across the pre and post-fire time-series (R^2 = 0.91–0.96 and RMSE = 3.41–7.30%) (Fig. 3). No under or over-estimation effects were observed for the entire range of vegetation cover measured in the field for each ecosystem, even in immediately post-fire environmental conditions, as shown in Fig. 3. The physically-based FVC retrieval scheme clearly outperformed the VIs approach used for benchmarking purposes. The FVC estimation from VIs provided a R^2 = 0.74–0.85 and a RMSE = 7.07–11.42 as the mean performance scores of the out-of-fold predictions across the pre and post-fire time se-

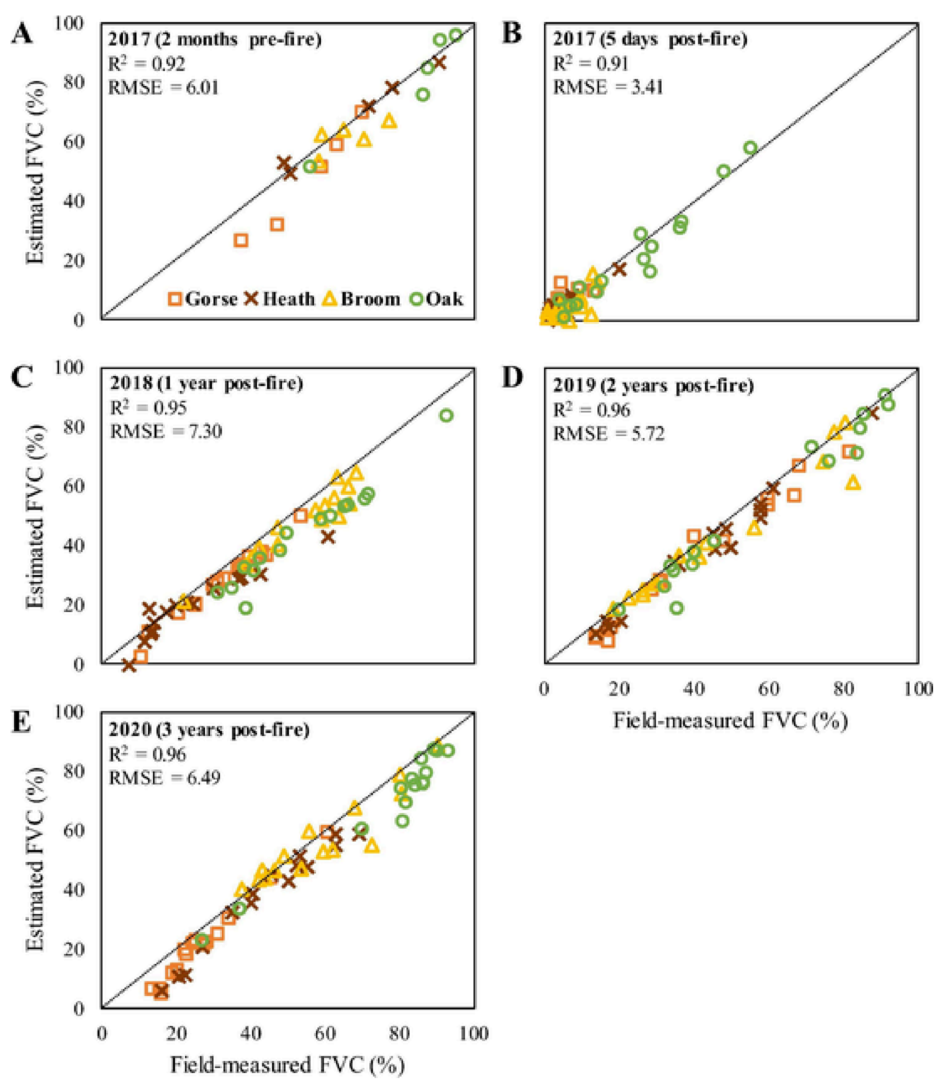

Fig. 3. Relationship between field-sampled and retrieved FVC from Deimos-2 imagery for the pre and post-fire time-series. The dotted line represents the regression (1):1 line.

ries. The three spectral indices featured a similar accuracy and prediction error (Table 6).

The impact of the fire disturbance on FVC was more pronounced ($p < 0.001$) under high burn severity in ecosystems dominated by tree species (i.e. oak and pine). For its part, the impact in shrub ecosystems (i.e. gorse, broom and heath) did not significantly differ between medium and high burn severity levels. Even in gorse ecosystem, the disturbance impact showed no significant differences between burn severity levels (Fig. 4 and Table SM1 of the Supplementary material).

Ecosystem resilience was conditioned by both burn severity and regenerative strategy (resprouter, seeder or facultative seeder) of the dominant species (Fig. 4 and Table SM2 of the Supplementary material). In all ecosystems, FVC recovery depended on burn severity, as resulted from the significant interaction ($p < 0.001$) between severity and time in the 2w-rmANOVA. Ecosystems dominated by facultative seeder shrubs (i.e. gorse and broom) reached pre-fire FVC conditions three years after the disturbance in areas burned at low ($p = 0.755$) and medium ($p = 0.956$) burn severity. Nevertheless, in areas affected by high burn severity, post-fire and pre-fire FVC differed significantly ($p < 0.001$) throughout the time-series and, therefore, resilience has not been achieved at short-term. Ecosystems dominated by resprouter species recovered the pre-fire FVC values one year after the disturbance when burned at low severity ($p = 0.151$ and $p = 0.144$ for heat and oak ecosystems, respectively). However, the resilience of both ecosystems differed at medium and high burn severity. Heath shrub ecosystem fully recovered pre-fire FVC even at high burn severity ($p = 0.993$) three years after fire, while oak tree ecosystem required the same time to recover in areas burned at medium severity ($p = 0.943$). In pine ecosystem, dominated by an obligate seeder, the third year after fire was the earliest point in the time series in which no significant FVC differences ($p = 0.641$) were observed from pre-fire FVC, corresponding to areas affected by low burn severity.

Most of the burned area (61% of the total surface occupied by the four considered ecosystems; Fig. 5) reached the FVC engineering re-

Table 6
Performance of trained GPR models from field-measured FVC and vegetation indices.

	EVI		MSAVI2		NDVI	
	R^2	RMSE	R^2	RMSE	R^2	RMSE
2017 (2 months pre-fire)	0.85	8.03	0.82	8.60	0.79	9.23
2017 (5 days post-fire)	0.76	7.85	0.77	7.07	0.74	8.75
2018 (1 year post-fire)	0.80	9.19	0.78	8.90	0.81	8.86
2019 (1 year post-fire)	0.82	10.66	0.83	10.73	0.77	11.15
2020 (1 year post-fire)	0.78	11.31	0.78	10.54	0.74	11.42

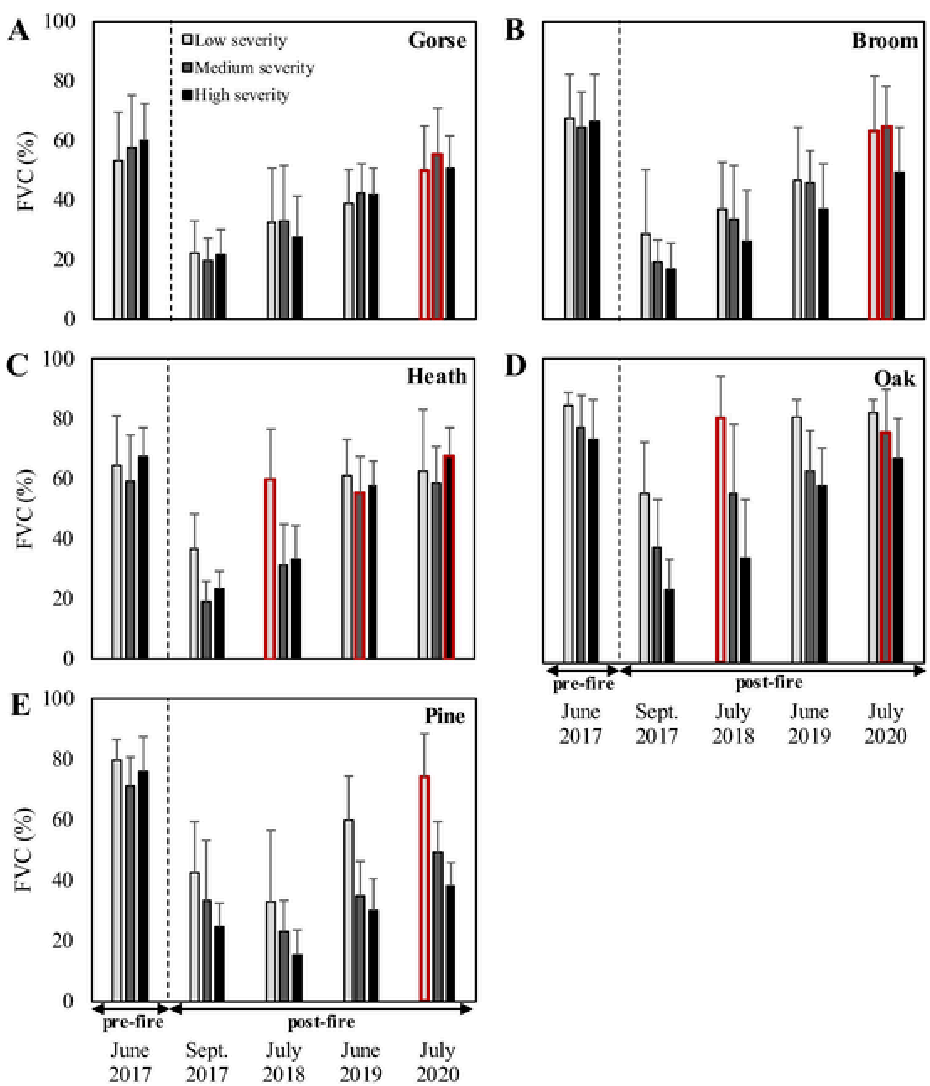

Fig. 4. Mean FVC and its standard deviation through the pre and post-fire time-series in gorse (A), broom (B), heath (C), oak (D) and pine (E) ecosystems. Columns with red border denote the earliest point in the time-series for which the FVC does not differ significantly at 0.05 level from the pre-fire FVC for a given burn severity level. (For interpretation of the references to colour in this figure legend, the reader is referred to the web version of this article.)

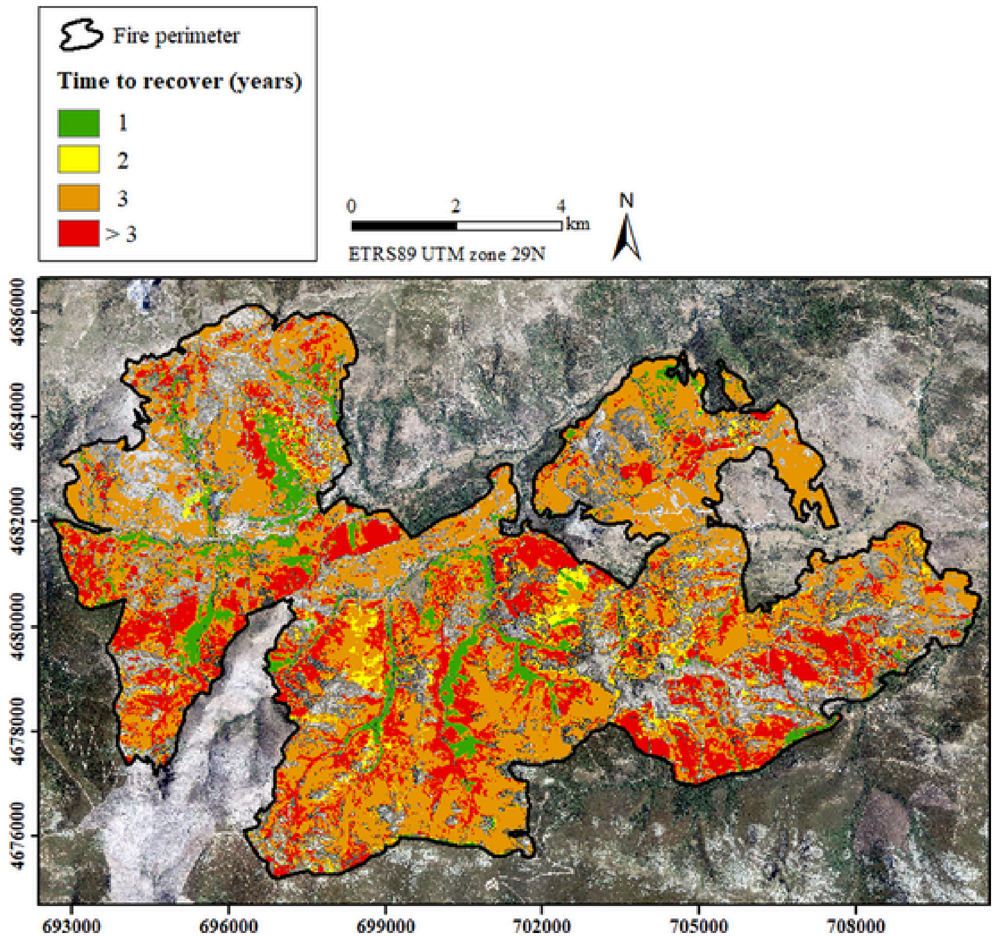

Fig. 5. Time to recover pre-fire FVC in the ecosystems affected by the fire disturbance. Blank areas within the wildfire perimeter correspond to ground cover not affected by the wildfire (e.g. rocks, tracks or crop areas).

silience three years after the wildfire. The 29% of the burned area did not reach pre-fire FVC values under any burn severity scenario during the analyzed time-series, and only the 10% of the area fully recovered its FVC one or two years after the fire.

4. Discussion

Monitoring post-fire recovery trends through remote sensing-based estimates is essential to determine engineering resilience at ecosystem, landscape and regional spatial scales (Díaz-Delgado et al., 2002; Fernandez-Manso et al., 2016; Meng et al., 2017; Yang et al., 2017; Meng et al., 2018; Fernández-Guisuraga et al., 2020), particularly in the context of changing fire regimes in Mediterranean ecosystems (González-De Vega et al., 2016; Vilà-Cabrera et al., 2018). The remote sensing-based tool developed in this study allowed for a reliable assessment of ecosystem resilience at short-term after fire, mainly due to the next facts: (i) The RTM hybrid inversion method has a good ability to generalize results, given its physical basis (Atzberger et al., 2015; He et al., 2020). (ii) The approach does not need the application of transferability analyses that require high field survey efforts (Vila and Barbosa, 2010; Fernández-Guisuraga et al., 2019). To minimize the reliance on field data is very relevant, since site-specific field data might not be available for scientists and land managers with the required quality and representativeness in extensive burned areas (Atzberger et al., 2015; Fernández-Guisuraga et al., 2021).

In this study, errors in FVC estimation were below the 10% threshold, which is considered as an acceptable standard (Drusch et al., 2012), particularly in post-fire immediate situation (five days' post-fire), with sparse photosynthetic material and abundant burned vegetation legacies exposed to the satellite sensor. The representative characterization of soil and non-photosynthetic material background signal extracted from Deimos-2 imagery in the training dataset of simulated canopy reflectance by PROSAIL-D could have improved the GPR model inversion to retrieve FVC (Verrelst et al., 2007). Also, the PROSPECT leaf RTM version chosen in this study (PROSPECT-D) simulates leaf reflectance and transmittance considering brown pigments and anthocyanins (Féret et al., 2017). Therefore, this leaf model could provide an added value in post-fire resilience studies at short-term, since these pigments are important constituents of leaves in post-fire environments under plant stress conditions (Gould, 2004). In addition, the evaluation of resilience to fire at ecosystem level should be based on remote sensing data at high spatial resolution, such as those used in this study. Otherwise, the fine-grained arrangement of vegetation legacies would not be captured in heterogeneous landscapes and the ecosystem regeneration resilience would be underestimated (Walker et al., 2019). This shortcoming could be partly solved by pixel unmixing modeling techniques that allow for obtaining fraction images of burned landscapes, which have also been widely used in the evaluation of post-fire recovery trajectories (e.g. Smith et al., 2007; Chu et al., 2016; Fernandez-Manso et al., 2016; Fernández-Guisuraga et al., 2020), even at the species level (Kibler et al., 2019). However, this approach requires the collection of an extensive spectral library (i.e. multiple endmembers for each ground component) to account for endmember variability caused by spatiotemporal changes in biophysical conditions of the different land cover types (Roberts et al., 1998; Somers et al., 2009), which is a challenge in extensive burned landscapes comprising several ecosystems. In addition, non-linear mixing caused by multiple scattering in sparse canopies violates the assumptions of the most used unmixing models, such as SMA or MESMA (Somers et al., 2009).

The performance of the RTM hybrid inversion method (R^2 = 0.91–0.96 and RMSE = 3.41–7.30%) was clearly superior to VIs approach (R^2 = 0.74–0.85 and RMSE = 7.07–11.42) for estimating FVC. Although VIs are correlated with certain biophysical properties of the canopy, these indices are not intrinsic physical quantities (Carlson and Ripley, 1997; Vila and Barbosa, 2010). Also, in burned areas with a great amount of non-photosynthetic material and soil background exposed to the remote sensors, VIs exhibit a larger error in the estimation of biophysical variables compared with physical-based approaches (Vila and Barbosa, 2010; Ding et al., 2017). Finally, canopy reflectance is not only governed by the vegetation amount estimated by VIs, but also by foliar chemistry and leaf angle distribution (Veraverbeke et al., 2012), used as input parameters in physical-based models. Hence, distinct ecosystem canopies in heterogeneous landscapes may yield different VIs values while exhibiting an identical FVC (Veraverbeke et al., 2012).

Remarkably, the results obtained by the RTM hybrid inversion method agreed with those achieved in previous studies based exclusively on in-situ field surveys, which proves the potential of the proposed remote sensing-based tool for assessing disturbance impact and ecosystem resilience at short-term. We found that, in tree forest ecosystems (i.e. oak and pine ecosystems), the fire impact on FVC was stronger at high burn severity, while in shrub ecosystems (i.e. gorse, broom and heath ecosystems) the impact was similar at medium and high burn severity, as found by Minor et al. (2017) in southeastern Arizona. Shrubs aboveground biomass is especially vulnerable to fire effects because of their low growth-form (Schwilk et al., 2013). In fact, even medium burn severity levels can significantly affect the shrub canopy and stems, as well as cambial tissues and roots due to convective heat (Pratt et al., 2014; Minor et al., 2017). Nevertheless, differentiation in medium and high burn severity impacts will presumably occur on the properties of other ecosystem compartments such as the soil. Despite the lack of significant differences in the disturbance impact on FVC across shrubland ecosystems affected by medium and high severity, engineering resilience was lower under high burn severity scenarios. Indeed, both the bud-forming tissues of resprouter species and the canopy or soil seed bank of seeders could be soundly affected by severe fires, reducing the resprouting vigor and seed recruitment, respectively (Pausas et al., 2003; Moreira et al., 2012; Maia et al., 2016; Strydom et al., 2020).

The faster recovery time that we have identified for resprouters-dominated ecosystems, in comparison with facultative or obligate seeders-dominated ecosystems, also agreed with previous research. Surviving tissues of resprouter species allow for a quick recovery of plant aboveground biomass (Pausas and Keeley, 2014b) and recolonization of the space occupied before the fire (Calvo et al., 2003; Vivian and Cary, 2012). This behavior confers to resprouters higher resilience than facultative or obligate seeders (Valdecantos et al., 2009; Chergui et al., 2018b). In fact, Vallejo and Alloza (1998) conclude that improved diversity and resilience could be achieved in post-fire landscapes through the promotion of shrub and tree resprouter formations. In a fire-prone burned landscape of the western Mediterranean Basin, Fernández-Guisuraga et al. (2020) found that areas dominated by resprouter shrubs and herbaceous species almost reached pre-fire vegetation cover four years after fire, whereas conifer stands dominated by obligate seeders, showed much lower post-fire recovery rates. The findings of Storey et al. (2016) and Kibler et al. (2019) in chamise chaparral shrublands in California, are also in agreement with the results of the present study regarding the recovery rates of resprouters and facultative or obligate seeders. Chergui et al. (2018b) also evidenced that several structure parameters of oak stands, dominated by resprouter species, were more resilient than those of conifer stands under a similar fire regime in a north-western Africa region with Mediterranean climatic conditions.

Likewise, burn severity hindered resilience to fire in all the ecosystems analyzed in this study, thus affecting both resprouting and seeding capacity (Vallejo et al., 2012; González-De Vega et al., 2016). This effect was more pronounced in ecosystems dominated by facultative or obligate seeders, where pre-fire FVC was reached later across the time-series compared to resprouter-dominated ecosystems, as the burn severity increased. In this sense, several research evidenced similar trait-dependent recovery patterns related to burn severity in Mediterranean ecosystems. Fernandez-Manso et al. (2016) found that only vegetation affected by low burn severity featured high resilience at short-term in a conifer stand of the western Mediterranean Basin. Heath et al. (2016) determined that increased burn severity delayed four years the short-term recovery to pre-fire spectral properties in several dry sclerophyll forests and shrubby woodlands dominated by resprouting vegetation in New South Wales, Australia. In contrast, several communities dominated by seeder species in the same region took much longer to recovery towards pre-wildfire conditions. In this sense, Díaz-Delgado et al. (2003) evidenced that burn severity had a more negative effect on the recovery time of shrub and forest stands dominated by seeders than of resprouters in a burned landscape of the western Mediterranean Basin.

Despite the advantages of using an engineering resilience indicator retrieved from optical satellite reflectance data, a primary limitation of this approach lies in the impossibility of determining ecosystem species composition and vertical structure parameters to identify the recovery trends of specific vegetation types within the ecosystem (Meng et al., 2015). In this sense, airborne multispectral LiDAR or data fusion of multispectral imagery with single-wavelength LiDAR (e.g. Kane et al., 2014; McCarley et al., 2017) could provide valuable information regarding post-fire recovery trajectories at species or growth form levels throughout the vertical vegetation profile in multi-layered canopies. However, in extensive burned areas, the high cost of LiDAR data collection (Hummel et al., 2011) restricts its use for evaluating forest resilience to fire. In addition, spectral unmixing techniques (e.g. MESMA) or object-based image classification of optical satellite imagery, may provide a reliable estimation of post-fire recovery trajectories considering species composition in ecosystems with single vegetation strata, or in multi-layered ecosystems at stand level (Mitri and Fiorucci, 2012; Kibler et al., 2019). Nevertheless, compositional attributes in multi-layered canopies cannot be directly retrieved with passive optical data on those strata that would normally be occluded by the top of canopy layer (Morsdorf et al., 2010; Vogeler and Cohen, 2016).

Regardless of the limitations of the FVC retrieval through a RTM hybrid inversion approach for evaluating resilience to fire, this technique may provide at short-term the operational needs to identify areas where intervention is necessary for assisting vegetation recovery and controlling soil erosion processes or nutrient losses. This approach should be further evaluated in the medium and long-term post-fire monitoring of forest resilience in order to examine whether the remote sensing-based observed patterns are still consistent with field observations.

5. Conclusions

The proposed remote sensing tool, based on the hybrid inversion of radiative transfer models (RTMs) to retrieve fractional vegetation cover (FVC) at high spatial resolution, has proved its reliability and applicability to monitor ecosystem engineering resilience in heterogeneous burned landscapes affected by mixed severity wildfires. The approach is computationally efficient to evaluate forest resilience in fire-prone landscapes at short-term and large spatial extent, minimizing the reliance on field data. In fact, the FVC retrieval over the entire pre and post-fire time-series was highly accurate despite the influence of the background signal of soil and burned legacies. The obtained results agree with previous field-based research in the sense that burn severity hinder ecosystem resilience, being detected quicker recovery to pre-fire

FVC state in ecosystems dominated by resprouters than facultative or obligate seeders at the lowest burn severity scenarios.

Uncited references

.

Declaration of Competing Interest

The authors declare that they have no known competing financial interests or personal relationships that could have appeared to influence the work reported in this paper.

Acknowledgements

This study was financially supported by the Spanish Ministry of Economy and Competitiveness, and the European Regional Development Fund (ERDF), in the framework of the GESFIRE (AGL2013-48189-C2-1-R) and FIRESEVES (AGL2017-86075-C2-1-R) projects; and by the Regional Government of Castilla and León in the framework of the FIRECYL (LE033U14), SEFIRECYL (LE001P17) and WUIFIRECYL (LE005P20) projects. J.M. Fernández-Guisuraga is supported by a predoctoral fellowship from the Spanish Ministry of Education (FPU16/03070). The authors would like to thank Deimos Imaging SLU for the Deimos-2 imagery provided.

References

Abdul-Malak, D., Pausas, J.G., Pardo-Pascual, J.E., Ruiz, L.A., 2015. Recurrence and the dynamics of the enhanced vegetation index in a Mediterranean ecosystem. Int. J. Appl. Geospatial Res. 6, 18–35.

Anderson, S., Anderson, W., Hines, F., Fountain, A., 2005. Determination of field sampling methods for the assessment of curing levels in grasslands. Bushfire Cooperative Research Centre, Project A1.4 Report.

Andrade, D., Ruschel, A.R., Schwartz, G., Carvalho, J., Humphries, S., Gama, J., 2020. Forest resilience to fire in eastern Amazon depends on the intensity of pre-fire disturbance. For. Ecol. Manage. 472, 118258.

Atzberger, C., Darvishzadeh, R., Immitzer, M., Schlerf, M., Skidmore, A., le Maire, G., 2015. Comparative analysis of different retrieval methods for mapping grassland leaf area index using airborne imaging spectroscopy. Int. J. Appl. Earth Obs. Geoinf. 43, 19–31.

Avitabile, V., Baccini, A., Friedl, M.A., Schmullius, C., 2012. Capabilities and limitations of Landsat and land cover data for aboveground woody biomass estimation of Uganda. Remote Sens. Environ. 117, 366–380.

Baret, F., Hagolle, O., Geiger, B., Bicheron, P., Miras, B., Huc, M., Berthelot, B., Niño, F., Weiss, M., Samain, O., Roujean, J.L., Leroy, M., 2007. LAI, fAPAR and fCover CYCLOPES global products derived from VEGETATION: Part 1: Principles of the algorithm. Remote Sens. Environ. 110, 275–286.

Bastos, A., Gouveia, C.M., DaCamara, C.C., Trigo, R.M., 2011. Modelling post-fire vegetation recovery in Portugal. Biogeosciences 8, 3593–3607.

Calvo, L., Santalla, S., Marcos, E., Valbuena, L., Tárrega, R., Luis, E., 2003. Regeneration after wildfire in one community dominated by obligate seeder Pinus pinaster and in another dominated by a typical resprouter Quercus pyrenaica. For. Ecol. Manage. 184, 209–223.

Calvo, L., Santalla, S., Valbuena, L., Marcos, E., Tárrega, R., Luis-Calabuig, E., 2008. Post-fire natural regeneration of a Pinus pinaster forest in NW Spain. Plant Ecol. 197, 81–90.

Campos-Taberner, M., Moreno-Martínez, Á., García-Haro, F.J., Camps-Valls, G., Robinson, N.P., Kattge, J., Running, S.W., 2018. Global Estimation of Biophysical Variables from Google Earth Engine Platform. Remote Sensing 10, 1167.

Carlson, T.N., Ripley, D.A., 1997. On the relation between NDVI, fractional vegetation cover, and Leaf Area Index. Remote Sens. Environ. 62, 241–252.

Carpenter, S.R., Westley, F., Turner, M.G., 2005. Surrogates for resilience of social-ecological systems. Ecosystems 8, 941–944.

Chergui, B., Fahd, S., Santos, X., Pausas, J.G., 2018a. Socioeconomic factors drive fire regime variability in the Mediterranean Basin. Ecosystems 21, 619–628.

Chergui, B., Fahd, S., Santos, X., 2018b. Quercus suber forest and Pinus plantations show different post-fire resilience in Mediterranean north-western Africa. Ann. Forest Sci. 75, 64.

Chergui, B., Fahd, S., Santos, X., 2019. Are reptile responses to fire shaped by forest type and vegetation structure? Insights from the Mediterranean basin. For. Ecol. Manage. 437, 340–347.

Chu, T., Guo, X., Takeda, K., 2016. Remote sensing approach to detect post-fire vegetation regrowth in Siberian boreal larch forest. Ecol. Ind. 62, 32–46.

Clemente, R., Navarro-Cerrillo, R., Gitas, I., 2009. Monitoring post-fire regeneration in Mediterranean ecosystems by employing multitemporal satellite imagery. Int. J. Wildland Fire 18, 648–658.

Darvishzadeh, R., Skidmore, A., Schlerf, M., Atzberger, C., 2008. Inversion of a radiative transfer model for estimating vegetation LAI and chlorophyll in a heterogeneous grassland. Remote Sens. Environ. 112, 2592–2604.

Davis, C.S., 2002. Statistical Methods for the Analysis of Repeated Measurements. Springer, New York, United States.

Delamater, P.L., Messina, J.P., Mark, J.K., Cochrane, A., 2012. A hybrid visual estimation method for the collection of ground truth fractional coverage data in a humid tropical environment. Int. J. Appl. Earth Obs. Geoinf. 18, 504–514.

Díaz-Delgado, R., Lloret, F., Pons, X., Terradas, J., 2002. Satellite evidence of decreasing resilience in Mediterranean plant communities after recurrent wildfires. Ecology 83, 2293–2303.

Díaz-Delgado, R., Lloret, F., Pons, X., 2003. Influence of fire severity on plant regeneration by means of remote sensing imagery. Int. J. Remote Sens. 24, 1751–1763.

Ding, Y., Zhang, H., Li, Z., Xin, X., Zheng, X., Zhao, K., 2016. Comparison of fractional vegetation cover estimations using dimidiate pixel models and look-up table inversions of the PROSAIL model from Landsat 8 OLI data. J. Appl. Remote Sens. 10, 036022.

Ding, Y., Zhang, H., Zhao, K., Zheng, X., 2017. Investigating the accuracy of vegetation index-based models for estimating the fractional vegetation cover and the effects of varying soil backgrounds using in situ measurements and the PROSAIL model. Int. J. Remote Sens. 38, 4206–4223.

Drusch, M., Del Bello, U., Carlier, S., Colin, O., Fernandez, V., Gascon, F., Hoersch, F., Isola, C., Laberinti, P., Martimort, P., Meygret, A., Spoto, F., Sy, O., Marchese, F., Bargellini, P., 2012. Sentinel-2: ESA's optical high-resolution mission for GMES operational services. Remote Sens. Environ. 120, 25–36.

Féret, J.B., Gitelson, A.A., Noble, S.D., Jacquemoud, S., 2017. PROSPECT-D: Towards modeling leaf optical properties through a complete lifecycle. Remote Sens. Environ. 193, 204–215.

Fernández-García, V., Santamarta, M., Fernández-Manso, A., Quintano, C., Marcos, E., Calvo, L., 2018. Burn severity metrics in fire-prone pine ecosystems along a climatic gradient using Landsat imagery. Remote Sens. Environ. 206, 205–217.

Fernández-Guisuraga, J.M., Calvo, L., Fernández-García, V., Marcos-Porras, E., Taboada, A., Suárez-Seoane, S., 2019. Efficiency of remote sensing tools for post-fire management along a climatic gradient. For. Ecol. Manage. 433, 553–562.

Fernández-Guisuraga, J.M., Calvo, L., Suárez-Seoane, S., 2020. Comparison of pixel unmixing models in the evaluation of post-fire forest resilience based on temporal series of satellite imagery at moderate and very high spatial resolution. ISPRS J. Photogramm. Remote Sens. 164, 217–228.

Fernández-Guisuraga, J.M., Verrelst, J., Calvo, L., Suárez-Seoane, S., 2021. Hybrid inversion of radiative transfer models based on high spatial resolution satellite reflectance data improves fractional vegetation cover retrieval in heterogeneous ecological systems after fire. Remote Sens. Environ. 255C, 112304.

Fernandez-Manso, A., Quintano, C., Roberts, D.A., 2016. Burn severity influence on post-fire vegetation cover resilience from Landsat MESMA fraction images time series in Mediterranean forest ecosystems. Remote Sens. Environ. 184, 112–123.

Franklin, J.F., Lindenmayer, D.B., MacMahon, J.A., McKee, A., Magnusson, J., Perry, D.A., Waide, R., Foster, D.R., 2000. Threads of continuity: ecosystem disturbances, biological legacies and ecosystem recovery. Conservt. Biol. Theory Pract. 1, 8–16.

Gao, X., Huete, A.R., Ni, W., Miura, T., 2000. Optical-biophysical relationships of vegetation spectra without background contamination. Remote Sens. Environ. 74, 609–620.

García-Haro, F.J., Campos-Taberner, M., Muñoz-Marí, J., Laparra, V., Camacho, F., Sánchez-Zapero, J., Camps-Valls, G., 2018. Derivation of global vegetation biophysical parameters from EUMETSAT Polar System. ISPRS J. Photogramm. Remote Sens. 139, 57–74.

García-Llamas, P., Suárez-Seoane, S., Fernández-Guisuraga, J.M., Fernández-García, V., Fernández-Manso, A., Quintano, C., Taboada, A., Marcos, E., Calvo, L., 2019. Evaluation and comparison of Landsat 8, Sentinel-2 and Deimos-1 remote sensing indices for assessing burn severity in Mediterranean fire-prone ecosystems. Int. J. Appl. Earth Obs. Geoinf. 80, 137–144.

García-Llamas, P., Suárez-Seoane, S., Fernández-Manso, A., Quintano, C., Calvo, L., 2020. Evaluation of fire severity in fire prone-ecosystems of Spain under two different environmental conditions. J. Environ. Manage. 271, 110706.

GEODE, 2019. Mapa Geológico Digital continuo de España. http://mapas.igme.es/gis/services/Cartografia_Geologica/IGME_Geode_50/MapServer/WMSServer/ (accessed 20 November 2020).

González-De Vega, S., De las Heras, J., Moya, D., 2016. Resilience of Mediterranean terrestrial ecosystems and fire severity in semiarid areas: Responses of Aleppo pine forests in the short, mid and long term. Sci. Total Environ. 573, 1171-1177.

Gould, K.S., 2004. Nature's Swiss Army Knife: The Diverse Protective Roles of Anthocyanins in Leaves. J. Biomed. Biotechnol. 5, 314–320.

Grimm, V., Calabrese, J.M., 2011. What is resilience? A short introduction. In: Deffuant, G., Gilbert, N. (eds) Viability and resilience of complex systems. Concepts, methods and case studies from ecology and society. Kluwer Academic Publishers, Dordrecht, pp. 3-16.

Gunderson, L.H., Holling, C.S., 2002. Panarchy: understanding transformations in human and natural systems. Island Press, Washington, United States.

He, Y., Yang, J., Guo, X., 2020. Green Vegetation Cover Dynamics in a

Heterogeneous Grassland: Spectral Unmixing of Landsat Time Series from 1999 to 2014. Remote Sensing 12, 3826.
Healey, S.P., Yang, Z., Gorelick, N., Ilyushchenko, S., 2020. Highly Local Model Calibration with a New GEDI LiDAR Asset on Google Earth Engine Reduces Landsat Forest Height Signal Saturation. Remote Sensing 12, 2840.
Heath, J.T., Chafer, C.J., Bishop, T.F.A., Ogtrop, F.F.V., 2016. Post-Fire Recovery of Eucalypt-Dominated Vegetation Communities in the Sydney Basin, Australia. Fire Ecol. 12, 53–79.
Holling, C.S., 1973. Resilience and stability of ecological systems. Annu. Rev. Ecol. Evol. Syst. 4, 1–23.
Hummel, S., Hudak, A.T., Uebler, E.H., Falkowski, M.J., Megown, K.A., 2011. A Comparison of Accuracy and Cost of LiDAR versus Stand Exam Data for Landscape Management on the Malheur National Forest. J. Forest. 109, 267–273.
Ingrisch, J., Bahn, M., 2018. Towards a Comparable Quantification of Resilience. Trends Ecol. Evol. 33, 251–259.
Ireland, G., Petropoulos, G.P., 2015. Exploring the relationships between post-fire vegetation regeneration dynamics, topography and burn severity: A case study from the Montane Cordillera Ecozones of Western Canada. Appl. Geogr. 56, 232–248.
ITACyL, 2019. Proyecto SUELOS. http://ftp.itacyl.es/Edafologia/ (accessed 20 November 2020).
Jacquemoud, S., Baret, F., 1990. PROSPECT: a model of leaf optical properties spectra. Remote Sens. Environ. 34, 75–91.
Jacquemoud, S., Verhoef, W., Baret, F., Bacour, C., Zarco-Tejada, P.J., Asner, G.P., François, C., Ustin, S.L., 2009. PROSPECT + SAIL models: A review of use for vegetation characterization. Remote Sens. Environ. 113, 56–66.
Jia, K., Liang, S., Gu, X., Baret, F., Wei, X., Wang, X., Yao, Y., Yang, L., Li, Y., 2016. Fractional vegetation cover estimation algorithm for Chinese GF-1 wide field view data. Remote Sens. Environ. 177, 184–191.
Jin, Y., Randerson, J.T., Goetz, S.J., Beck, P.S.A., Loranty, M.M., Goulden, M.L., 2012. The influence of burn severity on postfire vegetation recovery and albedo change during early succession in North American boreal forests. J. Geophys. Res. 117, G01036.
Johnstone, J.F., Allen, C.D., Franklin, J.F., Frelich, L.E., Harvey, B.J., Higuera, P. E., Mack, M.C., Meentemeyer, R.K., Metz, M.R., Perry, G.L.W., Schoennagel, T., Turner, M.G., 2016. Changing disturbance regimes, ecological memory, and forest resilience. Front. Ecol. Environ. 14, 369–378.
Kane, V.R., North, M.P., Lutz, J.A., Churchill, D.J., Roberts, S.L., Smith, D.F., McGaughey, R.J., Kane, J.T., Brooks, M.L., 2014. Assessing fire effects on forest spatial structure using a fusion of Landsat and airborne LiDAR data in Yosemite National Park. Remote Sens. Environ. 151, 89–101.
Kassambara, A., 2020. rstatix: Pipe-Friendly Framework for Basic Statistical Tests. R package version (6). https://CRAN.R-project.org/package=rstatix.
Kattge, J., et al., 2011. TRY-a global database of plant traits. Glob. Change Biol. 17, 2905–2935.
Keeley, J.E., 2009. Fire intensity, fire severity and burn severity: a brief review and suggested usage. Int. J. Wildland Fire 18, 116–126.
Keeley, J.E., Pausas, J.G., Rundel, P.W., Bond, W.J., Bradstock, R.A., 2011. Fire as an evolutionary pressure shaping plant traits. Trends Plant Sci. 16, 406–411.
Key, C.H., 2006. Ecological and sampling constraints on defining landscape fire severity. Fire Ecology 2, 34–59.
Key, C.H., Benson, N.C., 2006. Landscape Assessment (LA), in: Lutes, D.C., Keane, R.E., Caratti, J.F., Key, C.H., Benson, N.C., Sutherland, S., Gangi, L.J. (Eds.), FIREMON: Fire effects monitoring and inventory system. Gen. Tech. Rep. RMRS-GTR-164-CD. Department of Agriculture, Forest Service, Rocky Mountain Research Station, Fort Collins, United States, pp. 1-55.
Kibler, C.L., Parkinson, A.-M.L., Peterson, S.H., Roberts, D.A., D'Antonio, C.M., Meerdink, S.K., Sweeney, S.H., 2019. Monitoring Post-Fire Recovery of Chaparral and Conifer Species Using Field Surveys and Landsat Time Series. Remote Sensing 11, 2963.
Liang, S., Li, X., Wang, J., 2012. Advanced Remote Sensing: Terrestrial Information Extraction and Applications. Academic Press, Cambridge, United States.
Liang, L., Di, L., Zhang, L., Deng, M., Qin, Z., Zhao, S., Lin, H., 2015. Estimation of crop LAI using hyperspectral vegetation indices and a hybrid inversion method. Remote Sens. Environ. 165, 123–134.
Lozano, F.J., Suárez-Seoane, S., Kelly, M., Luis-Calabuig, E., 2008. A multi-scale approach for modeling fire occurrence probability using satellite data and classification trees: A case study in a mountainous Mediterranean region. Remote Sens. Environ. 112, 708–719.
Maia, P., Vasques, A., Pausas, J.G., Viegas, D.X., Keizer, J.J., 2016. Fire effects on the seed bank of three Mediterranean shrubs: implications for fire management. Plant Ecol. 217, 1235–1246.
Martin, S., Deffuant, G., Calabrese, J., 2011. Defining resilience mathematically: from attractors to viability. In: Deffuant, G., Gilbert, N. (Eds.), Viability and resilience of complex systems. Concepts, methods and case studies from ecology and society. Kluwer Academic Publishers, Dordrecht, pp. 17-48.
McCarley, T.R., Kolden, C.A., Vaillant, N.M., Hudak, A.T., Smith, A.M.S., Wing, B.M., Kellogg, B.S., Kreitler, J., 2017. Multi-temporal LiDAR and Landsat quantification of fire-induced changes to forest structure. Remote Sens. Environ. 191, 419–432.
McKay, M.D., Beckman, R.J., Conover, W.J., 1979. A Comparison of Three Methods for Selecting Values of Input Variables in the Analysis of Output from a Computer Code. Technometrics 21, 239–245.
Melendo-Vega, J.R., Martín, M.P., Pacheco-Labrador, J., González-Cascón, R., Moreno, G., Pérez, F., Migliavacca, M., García, M., North, P., Riaño, D., 2018. Improving the Performance of 3-D Radiative Transfer Model FLIGHT to Simulate Optical Properties of a Tree-Grass Ecosystem. Remote Sensing 10, 2061.
Melville, B., Fisher, A., Lucieer, A., 2019. Ultra-high spatial resolution fractional vegetation cover from unmanned aerial multispectral imagery. Int. J. Appl. Earth Obs. Geoinf. 78, 14–24.
Meng, R., Dennison, P.E., Huang, C., Moritz, M.A., D'Antonio, C., 2015. Effects of fire severity and post-fire climate on short-term vegetation recovery of mixed-conifer and red fir forests in the Sierra Nevada Mountains of California. Remote Sens. Environ. 171, 311–325.
Meng, R., Wu, J., Schwager, K.L., Zhao, F., Dennison, P.E., Cook, B.D., Brewster, K., Green, T.M., Serbin, S.P., 2017. Using high spatial resolution satellite imagery to map forest burn severity across spatial scales in a Pine Barrens ecosystem. Remote Sens. Environ. 191, 95–109.
Meng, R., Wu, J., Zhao, F., Cook, B.D., Hanavan, R.P., Serbin, S.P., 2018. Measuring short-term post-fire forest recovery across a burn severity gradient in a mixed pine-oak forest using multi-sensor remote sensing techniques. Remote Sens. Environ. 210, 282–296.
Merlin, M., Perot, T., Perret, S., Korboulewsky, N., Vallet, P., 2015. Effects of stand composition and tree size on resistance and resilience to drought in sessile oak and Scots pine. For. Ecol. Manage. 339, 22–33.
Minor, J., Falk, D.A., Barron-Gafford, G.A., 2017. Fire Severity and Regeneration Strategy Influence Shrub Patch Size and Structure Following Disturbance. Forests 8, 221.
Mitri, G., Fiorucci, P., 2012. Towards monitoring post-fire vegetation cover dynamics in the Mediterranean with the use of object-based image analysis of Landsat images. 1st EARSeL Workshop on Temporal Analysis of Satellite Images. Mykonos, Greece.
Moreira, B., Tormo, J., Pausas, J.G., 2012. To resprout or not to resprout: factors driving intraspecific variability in resprouting. Oikos 121, 1577–1584.
Morgan, P., Keane, R.E., Dillon, G.K., Jain, T.B., Hudak, A.T., Karau, E.C., Sikkink, P.G., Holden, Z.A., Strand, E.K., 2014. Challenges of assessing fire and burn severity using field measures, remote sensing and modelling. Int J. Wildland Fire 23, 1045–1060.
Morsdorf, F., Mårell, A., Koetz, B., Cassagne, N., Pimont, F., Rigolot, E., Allgöwer, B., 2010. Discrimination of vegetation strata in a multi-layered Mediterranean forest ecosystem using height and intensity information derived from airborne laser scanning. Remote Sens. Environ. 114, 1403–1415.
Mu, X., Huang, S., Ren, H., Yan, G., Song, W., Ruan, G., 2015. Validating GEOV1 fractional vegetation cover derived from coarse-resolution remote sensing images over croplands. IEEE J. Sel. Top. Appl. Earth Obs. Remote Sens. 8, 439–446.
Müller, F., Bergmann, M., Dannowski, R., Dippner, J.W., Gnauck, A., Haase, P., Jochimsen, M.C., Kasprzak, P., Kröncke, I., Kümmerlin, R., Küster, M., Lischeid, G., Meesenburg, H., Merz, C., Millat, G., Müller, J., Padisák, J., Schimming, C.G., Schubert, H., Schult, M., Selmeczy, G., Shatwell, T., Stoll, S., Schwabe, M., Soltwedel, T., Straile, D., Theuerkauf, M., 2016. Assessing resilience in long-term ecological data sets. Ecol. Ind. 65, 10–43.
Newton, A.C., Cantarello, E., 2015. Restoration of forest resilience: An achievable goal?. New Forest. 46, 645–668.
Nikinmaa, L., Lindner, M., Cantarello, E., Jump, A.S., Seidl, R., Winkel, G., Muys, B., 2020. Reviewing the Use of Resilience Concepts in Forest Sciences. Current Forestry Reports 6, 61–80.
[dataset] Ninyerola, M., Pons, X., Roure, J.M., 2005. Atlas Climático Digital de la Península Ibérica. Metodología y aplicaciones en bioclimatología y geobotánica. Universidad Autónoma de Barcelona.
Pausas, J.G., Ouadah, N., Ferran, A., Gimeno, T., Vallejo, R., 2003. Fire severity and seedling establishment in Pinus halepensis woodlands, eastern Iberian Peninsula. Plant Ecol. 169, 205–213.
Pausas, J.G., 2004. Changes in fire and climate in the Eastern Iberian Peninsula (Mediterranean Basin). Clim. Change 63, 337–350.
Pausas, J.G., Llovet, J., Rodrigo, A., Vallejo, R., 2008. Are wildfires a disaster in the Mediterranean basin? A review. Int. J. Wildland Fire 17, 713–723.
Pausas, J.G., Fernández-Muñoz, S., 2012. Fire regime changes in the Western Mediterranean Basin: from fuel-limited to drought-driven fire regime. Clim. Change 110, 215–226.
Pausas, J.G., Keeley, J.E., 2014a. Abrupt climate-independent fire regime changes. Ecosystems 17, 1109–1120.
Pausas, J.G., Keeley, J.E., 2014b. Evolutionary ecology of resprouting and seeding in fire-prone ecosystems. New Phytol. 204, 55–65.
Pimm, S.L., 1984. The complexity and stability of ecosystems. Nature 307, 321–326.
Pratt, R.B., Jacobsen, A.L., Ramirez, A.R., Helms, A.M., Traugh, C.A., Tobin, M. F., Heffner, M.S., Davis, S.D., 2014. Mortality of Resprouting Chaparral Shrubs after a Fire and during a Record Drought: Physiological Mechanisms and Demographic Consequences. Glob. Change Biol. 20, 893–907.
Qi, J., Chehbouni, A., Huete, A.R., Kerr, Y.H., 1994. Modified Soil Adjusted Vegetation Index (MSAVI). Remote Sens. Environ. 48, 119–126.
Rasmussen, C.E., Williams, C.K.I., 2006. Gaussian Processes for Machine Learning. The MIT Press, New York.
R Core Team, 2019. R: A language and environment for statistical computing. R Foundation for Statistical Computing, Vienna, Austria https://www.R-project.org/.
Reyer, C.P.O., Brouwers, N., Rammig, A., Brook, B.W., Epila, J., Grant, R.F., Holmgren, M., Langerwisch, F., Leuzinger, S., Lucht, W., Medlyn, B., Pfeifer,

M., Steinkamp, J., Vanderwel, M.C., Verbeeck, H., Villela, D.M., 2015. Forest resilience and tipping points at different spatio-temporal scales: approaches and challenges. J. Ecol. 103, 5–15.
Richter, R., Schläpfer, D., 2018. Atmospheric / Topographic Correction for Satellite Imagery. DLR Report DLR-IB 565-01/2018, Wessling, Germany.
Roberts, D.A., Gardner, M., Church, R., Ustin, S., Scheer, G., Green, R.O., 1998. Mapping Chaparral in the Santa Monica Mountains using Multiple Endmember Spectral Mixture Models. Remote Sens. Environ. 65, 267–279.
Rouse, J.W., Haas, R.H., Schell, J.A., Deering, D.W., 1979. Monitoring vegetation systems in the great plains with ERTS. Proceedings of the Third ERTS Symposium. NASA SP-351, 1, NASA, Washington DC, United states.
Sagra, J., Moya, D., Plaza-Álvarez, P.A., Lucas-Borja, M.E., González-Romero, J., De las Heras, J., Alfaro-Sánchez, R., Ferrandis, P., 2019. Prescribed fire effects on early recruitment of Mediterranean pine species depend on fire exposure and seed provenance. Forest Ecol. Manage., 441: 253-261.
Scheffer, M., Carpenter, S., Foley, J.A., Folke, C., Walker, B., 2001. Catastrophic shifts in ecosystems. Nature 413, 591–596.
Scheffer, M., Carpenter, S.R., Dakos, V., van Nes, E.H., 2015. Generic Indicators of Ecological Resilience: Inferring the Chance of a Critical Transition. Annu. Rev. Ecol. Evol. Syst. 46, 145–167.
Schlerf, M., Atzberger, C., 2006. Inversion of a forest reflectance model to estimate biophysical canopy variables from hyperspectral remote sensing data. Remote Sens. Environ. 100, 281–294.
Schwilk, D.W., Gaetani, M.S., Poulos, H.M., 2013. Oak Bark Allometry and Fire Survival Strategies in the Chihuahuan Desert Sky Islands, Texas, USA. PLoS ONE 8, e79285.
Seidl, R., Rammer, W., Spies, T.A., 2014. Disturbance legacies increase the resilience of forest ecosystem structure, composition, and functioning. Ecol. Appl. 24, 2063–2077.
Seidl, R., Spies, T.A., Peterson, D.L., Stephens, S.L., Hicke, J.A., 2016. Searching for resilience: addressing the impacts of changing disturbance regimes on forest ecosystem services. J. Appl. Ecol. 53, 120–129.
Sinha, S.K., Padalia, H., Dasgupta, A., Verrelst, J., Rivera, J.P., 2020. Estimation of leaf area index using PROSAIL based LUT inversion, MLRA-GPR and empirical models: Case study of tropical deciduous forest plantation, North India. Int. J. Appl. Earth Obs. Geoinf. 86, 102027.
Smith, A.M., Lentile, L.B., Hudak, A.T., Morgan, P., 2007. Evaluation of linear spectral unmixing and DNBR for predicting post-fire recovery in a North American ponderosa pine forest. Int. J. Remote Sens. 28, 5159–5166.
Somers, B., Cools, K., Delalieux, S., Stuckens, J., Van der Zande, D., Verstraeten, W.W., Coppin, P., 2009. Nonlinear Hyperspectral Mixture Analysis for tree cover estimates in orchards. Remote Sens. Environ. 113, 1183–1193.
Storey, E.A., Stow, D.A., O'Leary, J.F., 2016. Assessing postfire recovery of chamise chaparral using multi-temporal spectral vegetation index trajectories derived from Landsat imagery. Remote Sens. Environ. 183, 53–64.
Strydom, T., Kraaij, T., Difford, M., Cowling, R.M., 2020. Fire severity effects on resprouting of subtropical dune thicket of the Cape Floristic Region. PeerJ 8, e9240.
Taboada, A., Fernández-García, V., Marcos, E., Calvo, L., 2018. Interactions between large high-severity fires and salvage logging on a short return interval reduce the regrowth of fire-prone serotinous forests. For. Ecol. Manage. 414, 54–63.
Tao, G., Jia, K., Zhao, X., Wei, X., Xie, X., Zhang, X., Wang, B., Yao, Y., Zhang, X., 2019. Generating High Spatio-Temporal Resolution Fractional Vegetation Cover by Fusing GF-1 WFV and MODIS Data. Remote Sensing 11, 2324.
Tukey, J., 1949. Comparing Individual Means in the Analysis of Variance. Biometrics. 5, 99–114.
Turetsky, M.R., Baltzer, J.L., Johnstone, J.F., Mack, M.C., McCann, K., Schuur, E. A.G., 2017. Losing legacies, ecological release, and transient responses: key challenges for the future of northern ecosystem science. Ecosystems 20, 23–30.
Valdecantos, A., Baeza, M.J., Vallejo, V.R., 2009. Vegetation Management for Promoting Ecosystem Resilience in Fire-Prone Mediterranean Shrublands. Restor. Ecol. 17, 414–421.
Vallejo, V.R., Alloza, J.A., 1998. The restoration of burned lands: the case of Eastern Spain. In: Moreno, J.M. (Ed.), Large forest fires. Backhuys Publishers, Leiden, The Netherlands, pp. 91–108.
Vallejo, V.R., Arianoutsou, M., Moreira, F., 2012. Fire ecology and post-fire Restoration approaches in southern European forest types. In: Moreira, F., Arianoutsou, M., Corona, P., De Las Heras, J. (Eds.), Post-fire Management and Restoration of Southern European Forests. Springer, Netherlands, pp. 93–119.
van der Meer, F.D., de Jong, S.M., 2001. Imaging Spectrometry: Basic Principles and Prospective Applications. Springer, Netherlands.
Veraverbeke, S., Gitas, I., Katagis, T., Polychronaki, A., Somers, B., Goossens, R., 2012. Assessing post-fire vegetation recovery using red–near infrared vegetation indices: Accounting for background and vegetation variability. ISPRS J. Photogramm. Remote Sens. 68, 28–39.
Verhoef, W., Xiao, Q., Jia, L., Su, Z., 2007. Unified optical-thermal four-stream radiative transfer theory for homogeneous vegetation canopies. IEEE Trans. Geosci. Remote Sens. 45, 1808–1822.
Verrelst, J., Zurita-Milla, R., Koetz, B., Clevers, J.G.P.W., Schaepman, M.E., 2007. Angular unmixing of photosynthetic and non-photosynthetic vegetation within a coniferous forest using CHRIS-PROBA, Proceedings of the 10th International Symposium on Physical Measurements and Spectral Signatures in Remote Sensing, 36: 355-360.
Verrelst, J., Alonso, L., Camps-Valls, G., Delegido, J., Moreno, J., 2012a. Retrieval of Vegetation Biophysical Parameters Using Gaussian Process Techniques. IEEE Trans. Geosci. Remote Sens. 50, 1832–1843.
Verrelst, J., Muñoz, J., Alonso, L., Delegido, J., Rivera, J.P., Camps-Valls, G., Moreno, J., 2012b. Machine learning regression algorithms for biophysical parameter retrieval: Opportunities for Sentinel-2 and -3. Remote Sens. Environ. 118, 127–139.
Verrelst, J., Romijn, E., Kooistra, L., 2012c. Mapping vegetation structure in a heterogeneous river floodplain ecosystem using pointable CHRIS/PROBA data. Remote Sensing 4, 2866–2889.
Verrelst, J., Rivera, J.P., Veroustraete, F., Muñoz-Marí, J., Clevers, J.G.P.W., Camps-Valls, G., Moreno, J., 2015. Experimental Sentinel-2 LAI estimation using parametric, non-parametric and physical retrieval methods – A comparison. ISPRS J. Photogramm. Remote Sens. 108, 260–272.
Verrelst, J., Rivera, J.P., Gitelson, A., Delegido, J., Moreno, J., Camps-Valls, G., 2016. Spectral band selection for vegetation properties retrieval using Gaussian processes regression. Int. J. Appl. Earth Obs. Geoinf. 52, 554–567.
Vicent, J., Verrelst, J., J.P., Rivera-Caicedo, Sabater, N., Muñoz-Marí, J., Camps-Valls, G., Moreno, J., 2018. Emulation as an Accurate Alternative to Interpolation in Sampling Radiative Transfer Codes. IEEE J. Selected Topics Appl. Earth Observ. Remote Sens. 11, 4918-4931.
Viedma, O., Melia, J., Segarra, D., Garcia-Haro, J., 1997. Modeling rates of ecosystem recovery after fires by using Landsat TM data. Remote Sens. Environ. 61, 383–398.
Vila, G., Barbosa, P., 2010. Post-fire vegetation regrowth detection in the Deiva Marina region (Liguria-Italy) using Landsat TM and ETM+ data. Ecol. Model. 221, 75–84.
Vilà-Cabrera, A., Coll, L., Martínez-Vilalta, J., Retana, J., 2018. Forest management for adaptation to climate change in the Mediterranean basin: A synthesis of evidence. For. Ecol. Manage. 407, 16–22.
Vivian, L.M., Cary, G.J., 2012. Relationship between leaf traits and fire-response strategies in shrub species of a mountainous region of south-eastern Australia. Ann. Bot. 109, 197–208.
Vogeler, J.C., Cohen, W.B, 2016. A review of the role of active remote sensing and data fusion for characterizing forest in wildlife habitat models. Revista de Teledetección 45, 1-14.
Walker, R.B., Coop, J.D., Downing, W.M., Krawchuk, M.A., Malone, S.L., Meigs, G.W., 2019. How Much Forest Persists Through Fire? High-Resolution Mapping of Tree Cover to Characterize the Abundance and Spatial Pattern of Fire Refugia Across Mosaics of Burn Severity. Forests 10, 782.
Wang, B., Jia, K., Liang, S., Xie, X., Wei, X., Zhao, X., Yao, Y., Zhang, X., 2018. Assessment of Sentinel-2 MSI Spectral Band Reflectances for Estimating Fractional Vegetation Cover. Remote Sensing 10, 1927.
Yang, J., Pan, S., Dangal, S., Zhang, B., Wang, S., Tian, H., 2017. Continental-scale quantification of post-fire vegetation greenness recovery in temperate and boreal North America. Remote Sens. Environ. 199, 277–290.
Yebra, M., Chuvieco, E., Riaño, D., 2008. Estimation of live fuel moisture content from MODIS images for fire risk assessment. Agric. For. Meteorol. 148, 523–536.
Yebra, M., Chuvieco, E., 2009. Linking ecological information and radiative transfer models to estimate fuel moisture content in the Mediterranean region of Spain: Solving the ill-posed inverse problem. Remote Sens. Environ. 113, 2403–2411.
Yi, K., Tani, H., Zhang, J., Guo, M., Wang, X., Zhong, G., 2013. Long-term satellite detection of post-fire vegetation trends in boreal forests of China. Remote Sensing 5, 6938–6957.
Younes, N., Joyce, K.E., Northfield, T.D., Maier, S.W., 2019. The effects of water depth on estimating Fractional Vegetation Cover in mangrove forests. Int. J. Appl. Earth Obs. Geoinf. 83, 101924.
Zhang, X., Liao, C., Li, J., Sun, Q., 2013. Fractional vegetation cover estimation in arid and semi-arid environments using HJ-1 satellite hyperspectral data. Int. J. Appl. Earth Obs. Geoinf. 21, 506–512.